Decoupling Perception and Calibration: Label-Efficient Image Quality Assessment Framework

Xinyue Li[1] , **Zhichao Zhang**[1] , **Zhiming Xu**[2] , **Shubo Xu**[3] , **Xiongkuo Min**[1] , **Yitong Chen**[1†] and **Guangtao Zhai**[1†]

[1]Shanghai Jiao Tong University, [2]Xi'an Jiaotong University, [3]Baidu
{xinyueli, liquortect}@sjtu.edu.cn, xzm060320@stu.xjtu.edu.cn, xushubo@baidu.com,
{minxiongkuo,yitongchen,zhaiguangtao}@sjtu.edu.cn

Abstract

Recent multimodal large language models (MLLMs) have demonstrated strong capabilities in image quality assessment (IQA) tasks. However, adapting such large-scale models is computationally expensive and still relies on substantial Mean Opinion Score (MOS) annotations. We argue that for MLLM-based IQA, the core bottleneck lies not in the quality perception capacity of MLLMs, but in MOS scale calibration. Therefore, we propose LEAF, a _Label-Efficient Image Quality Assessment Framework_ that distills perceptual quality priors from an MLLM teacher into a lightweight student regressor, enabling MOS calibration with minimal human supervision. Specifically, the teacher conducts dense supervision through point-wise judgments and pair-wise preferences, with an estimate of decision reliability. Guided by these signals, the student learns the teacher's quality perception patterns through joint distillation and is calibrated on a small MOS subset to align with human annotations. Experiments on both user-generated and AI-generated IQA benchmarks demonstrate that our method significantly reduces the need for human annotations while maintaining strong MOS-aligned correlations, making lightweight IQA practical under limited annotation budgets. The code will be released upon the publication.

1 Introduction

Image Quality Assessment (IQA) is a key component of modern visual systems, supporting a wide range of applications including camera calibration, image enhancement, content filtering, streaming media optimization, and large-scale data management [Fang _et al._, 2020; Seufert _et al._, 2014]. IQA facilitates efficient benchmarking and optimization of image enhancement and generative models by providing feedback that is consistent with human standards [Ding _et al._, 2022; Li _et al._, 2025; Zhang _et al._, 2023; Wang _et al._, 2023].

Multimodal large language models (MLLMs) have recently demonstrated outstanding capabilities in IQA tasks, often matching specialized IQA models by leveraging strong
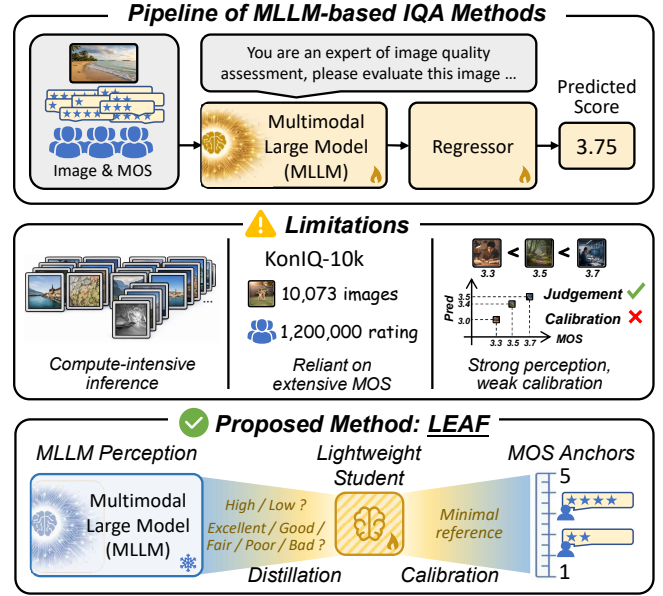

Figure 1: Using MLLMs for IQA is computationally expensive and annotation-intensive. MLLMs can perceive the key information of image quality. This work advocates decoupling quality perception from MOS calibration, thereby enabling efficient image quality assessment with minimal human supervision.

visual understanding and rich prior knowledge [Zhang _et al._, 2025; Wang _et al._, 2024; Wu _et al._, 2024]. This advancement has led to an emerging practice, treating MLLMs as high-performing quality evaluators and adapting them for IQA through instruction tuning or task-specific fine-tuning [Li _et al._, 2025; Wang _et al._, 2025a; Chen _et al._, 2024]. However, despite the considerable accuracy of these MLLM-based methods, they still face two practical barriers that limit their usability in real-world IQA pipelines, as shown in Figure 1.

First, MLLM-based methods are computationally expensive throughout the pipeline, both during training and at deployment[Wu _et al._, 2024]. For example, [Wang _et al._, 2025a] and [Xu _et al._, 2025] proposed MLLM-based IQA methods, which require training and inference on large memory GPUs. This makes large MLLMs difficult to use in settings that demand fast, low-cost, and scalable quality prediction, such as on-device assessment, large-scale data filtering,
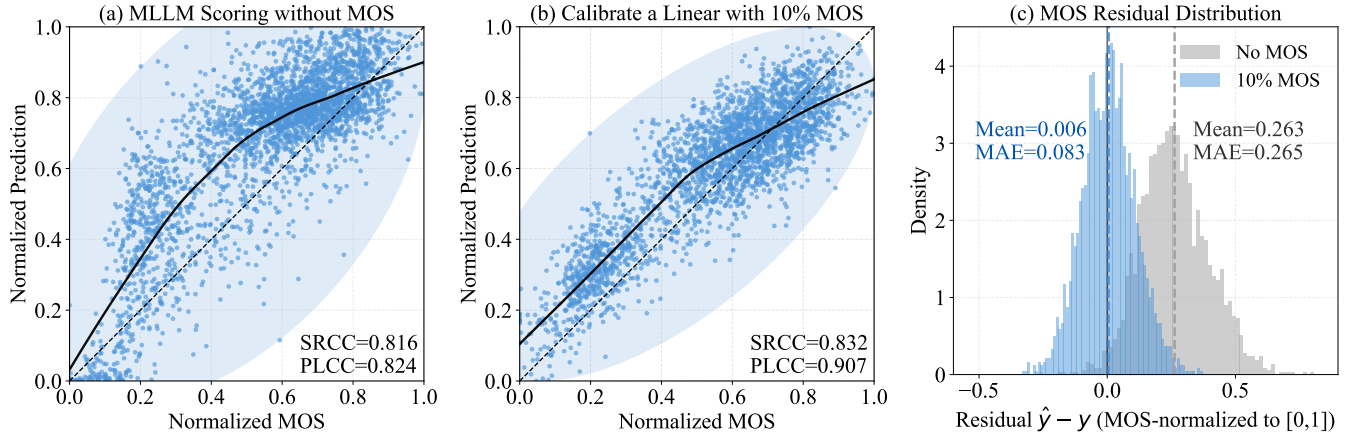
Figure 2: Direct MLLM scoring on AGIQA-3K exhibits strong monotonic correlation with MOS (SRCC=0.816) but suffers from pronounced scale bias and non-linear mapping (shown in (a)). Calibrating a Linear with only 10% MOS substantially improves MOS alignment (PLCC from 0.824 to 0.907) and reduces residual bias (mean residual from 0.263 to 0.006).

and real-time monitoring[Wu *et al.*, 2024].

Second, current IQA methods mainly rely on supervised learning with human mean opinion scores (MOS) [Li *et al.*, 2025; Wang *et al.*, 2024]. Although MOS can provide reliable subjective judgments under controlled protocols, MOS annotation is resource-intensive. For example, the KonIQ-10K [Hosu *et al.*, 2020] dataset contains more than $10,000$ images and has collected a total of 1.2 million opinion scores. Moreover, subjective quality perception drifts with the scenario. Therefore, MOS annotations need to be recollected as scenarios and time changes.

More importantly, for a pretrained MLLM, the primary limitation is often not the capability of quality perception, but the absence of explicit MOS scale calibration. Specifically, MLLMs perform well in capturing comparative and quality classification, such as distinguishing better versus worse images or assigning coarse quality levels. However, they struggle to map these perceptual judgments onto the MOS rating scales of specific datasets and specific scenarios.

Figure 2 illustrates this phenomenon on the AGIQA-3K dataset. Direct MLLM scoring preserves reliable ranking, but suffers from clear MOS scale miscalibration. Calibrating only a lightweight head with 10% MOS largely removes the residual bias and improves MOS alignment while keeping ranking performance (Fig. 2(b,c)). This suggests that the key challenge is MOS scale calibration rather than relearning perception. Consequently, directly fine-tuning MLLMs using large-scale MOS annotations is an inefficient strategy. More experimental details are reported in the supplementary materials.

Inspired by this observation, in this work, we answer this question with **LEAF**, a *Label-Efficient Image Quality Assessment Framework* that transfers perceptual quality knowledge from an MLLM teacher into a lightweight student. The key idea is to use the teacher to provide dense supervision on a large unlabeled image set, and reserve human MOS labels only for final calibration.

Concretely, the teacher provides two complementary forms of supervision: (i) **point-wise** quality judgments for individual images, and (ii) **pair-wise** preferences that encode relative quality rankings, and also include estimates of decision reliability. Leveraging these signals, we formulate a Joint Teacher-Guided Distillation to enable the student to learn the teacher's quality perception. We then conduct Calibration Fine-Tuning on only a small MOS subset to align the student's scoring scale with human judgments.

Our contributions are summarized as follows:

- We formulate a label-efficient IQA framework that decouples perceptual knowledge from MOS calibration, based on the insight that MLLMs are strong at quality perception but weak at dataset-specific MOS alignment.

- We propose a two-stage teacher-guided framework that transfers perceptual quality priors to a lightweight student by joint distillation of point-wise judgments and confidence-weighted pair-wise preferences, followed by calibration using a small MOS-labeled subset.

- Experiments on both UGC and AIGC benchmarks validate the proposed decoupling principle, showing that strong MOS-aligned correlation can be achieved with limited MOS supervision, while avoiding costly task-specific fine-tuning of MLLMs.

2 Related Work

2.1 Image Quality Assessment

Handcrafted IQA

Early image quality assessment (IQA) relied on handcrafted fidelity and perception priors, among which SSIM-style structural comparison methods became influential and were further extended to improve robustness under diverse distortions [Wang *et al.*, 2003]. Complementary handcrafted cues were explored through phase and gradient features to better capture perceptually significant structural changes [Zhang *et al.*, 2011]. No-reference IQA subsequently adopted natural scene statistics to treat distortions as a deviation from

natural regularities, as demonstrated by DIIVINE [Moorthy and Bovik, 2011], BRISQUE [Mittal *et al.*, 2012a], and the opinion-unaware NIQE [Mittal *et al.*, 2012b].

Deep Learning–based IQA

Deep IQA learns quality-aware representations directly from data, while WaDIQaM [Bosse *et al.*, 2016] is an early blind image quality assessment model based on CNN. Full-reference IQA also shifted to deep feature distances, such as LPIPS [Zhang *et al.*, 2018], DISTS [Ding *et al.*, 2022], and PieAPP [Prashnani *et al.*, 2018]. Later blind IQA methods improved adaptability and spatial sensitivity through hypernetworks in HyperIQA [Su *et al.*, 2020], attention mechanisms [Chen *et al.*, 2020], pseudo-reference hallucination in HIQA [Lin and Wang, 2018], and stronger CNN interactions [Zhang *et al.*, 2020], while transformers such as MUSIQ [Ke *et al.*, 2021] and MANIQA [Yang *et al.*, 2022] further strengthen global and multi-scale modeling.

Multi-modal Model-based IQA

Multimodal IQA exploits vision-language priors, where LIQE [Zhang *et al.*, 2023] combines image and text embeddings and CLIP-IQA [Wang *et al.*, 2023] supports prompt-based zero-shot assessment. For AI-generated images, prompt consistency can be explicitly modeled within the CLIP-based frameworks, and multimodal large models can also provide discrete judgments and continuous scoring for quality assessment [Fu *et al.*, 2024; Zhang *et al.*, 2025]. Recent AIGC-IQA frameworks include MA-AGIQA [Wang *et al.*, 2024] and SEAGULL [Chen *et al.*, 2024], while Evo-Quality [Wen *et al.*, 2025] explore zero-shot or self-evolving ranking strategies, and AGHI-QA [Li *et al.*, 2025] provides a dedicated benchmark, but most methods still rely on annotation and motivate label-free alternatives.

2.2 Label-Free IQA Methods

Classical NSS-based Model

Although supervised IQA achieves strong performance, collecting large-scale MOS labels is costly and difficult to scale to new domains and rapidly evolving AI-generated content. This motivates the emergence of label-free IQA, which estimates perceptual quality without explicit MOS supervision. Early methods follow the NIQE-style paradigm, they model pristine natural-scene statistics and quantify quality by the deviations from learned priors, e.g., NIQE [Mittal *et al.*, 2012b], IL-NIQE [Zhang *et al.*, 2015], and uBIQA [Xue *et al.*, 2013]. This idea has been further extended to domain-specific scenarios such as medical IQA (MSM-MIQ [Yuan *et al.*, 2024]).

Deep Distribution Model

Beyond the hand-crafted NSS method, deep distribution modeling aims to better characterize high-quality image priors. MDFS [Ni *et al.*, 2024] learns multi-scale deep feature distributions, while DSTS [Li *et al.*, 2024b] separates shape- and texture-biased representations to capture various degradation scenarios. Generative and self-supervised variants learn quality-related latent spaces or features for deviation-based scoring, such as adversarial CVAE-based opinion-unaware perceptual IQA [Shukla *et al.*, 2024] and NROUQA [Babu *et al.*, 2023]. Despite different implementation approaches,

these methods remain largely consistent with the NIQE-style principle of deviation from the original state.

Pretraining and Quality Representation

Another line focuses on achieving label-free quality-aware representation learning through self-supervised or pretext-based objectives. QPT [Zhao *et al.*, 2023] introduced quality-aware contrastive pretraining, ARNIQA [Agnolucci *et al.*, 2024], and CONTRIQUE [Madhusudana *et al.*, 2022] utilized synthetic degradation sequences and distortion-conditioned contrastive learning. Transformer-based designs further combine contrastive learning with quality regression [Shi *et al.*, 2024], while Re-IQA [Saha *et al.*, 2023] used a dual encoder to separate content and quality. DUBMA [Wang *et al.*, 2025b] leverages a large distortion bank and FR-IQA evaluation metrics as pseudo-annotators for ranking supervision, and QualiCLIP [Agnolucci *et al.*, 2025] aligned degraded images with quality-related antonymic prompts to learn multimodal embeddings while avoiding the use of MOS.

3 Method

3.1 Overview

To reduce the reliance on large-scale human MOS annotations while maintaining MOS-aligned IQA performance, we propose **LEAF**, a *L̲abel-E̲fficient Image Quality A̲ssessment F̲ramework* with two components: (i) *Teacher-Guided Distillation* that produces point-wise judgment and pair-wise preferences, and the student learns from dense teacher signals without using MOS in the distillation objective at stage 1, and (ii) *Calibration Fine-Tuning* that calibrates the student model using a small MOS subset at stage 2. An overview is shown in Figure 3.

Let $\mathcal{D} = \{x_i\}_{i=1}^N$ be a set of training images, and let only a small subset $\mathcal{D}_{\mathrm{MOS}} = \{(x_i, y_i)\}_{i=1}^M \subset \mathcal{D}$ be annotated with human MOS $y_i \in \mathbb{R}$, where $M \ll N$. Our goal is to learn a lightweight student regressor $s_\theta : \mathcal{X} \rightarrow \mathbb{R}$ that predicts perceptual quality scores aligned with MOS.

Teacher-Guided Distillation

Given an image $x \in \mathcal{D}$, the MLLM teacher provides: (i) a point-wise judgment $\hat{y}^T(x)$, and (ii) a set of pair-wise supervision tuples $\mathcal{P} = \{(x_a, x_b, t_{ab}, \omega_{ab})\}$ with $(x_a, x_b) \in \mathcal{D} \times \mathcal{D}$. We construct $\mathcal{P}$ by uniformly sampling image pairs at random from $\mathcal{D} \times \mathcal{D}$. For each pair, we assign x_a as option A and x_b as option B in the teacher prompt. Here $t_{ab} \in \{0, 1\}$ indicates the teacher's preference, where $t_{ab} = 1$ if x_a is judged to have higher quality than x_b, and $\omega_{ab} \in [0, 1]$ measures the confidence of this decision.

During this stage, student s_θ is trained through dense teacher-induced supervision, without using MOS labels in the distillation objective. Concretely, the student is optimized to (i) match the teacher's point-wise judgment $\hat{y}^T(x)$ and (ii) preserve the pairwise ranking induced by the teacher, weighted by the teacher's confidence encoded in $\mathcal{P}$.

Calibration Fine-Tuning

This stage uses the small MOS-labeled subset $\mathcal{D}_{\mathrm{MOS}}$ to calibrate the student predictions to the MOS scale. We fine-tune
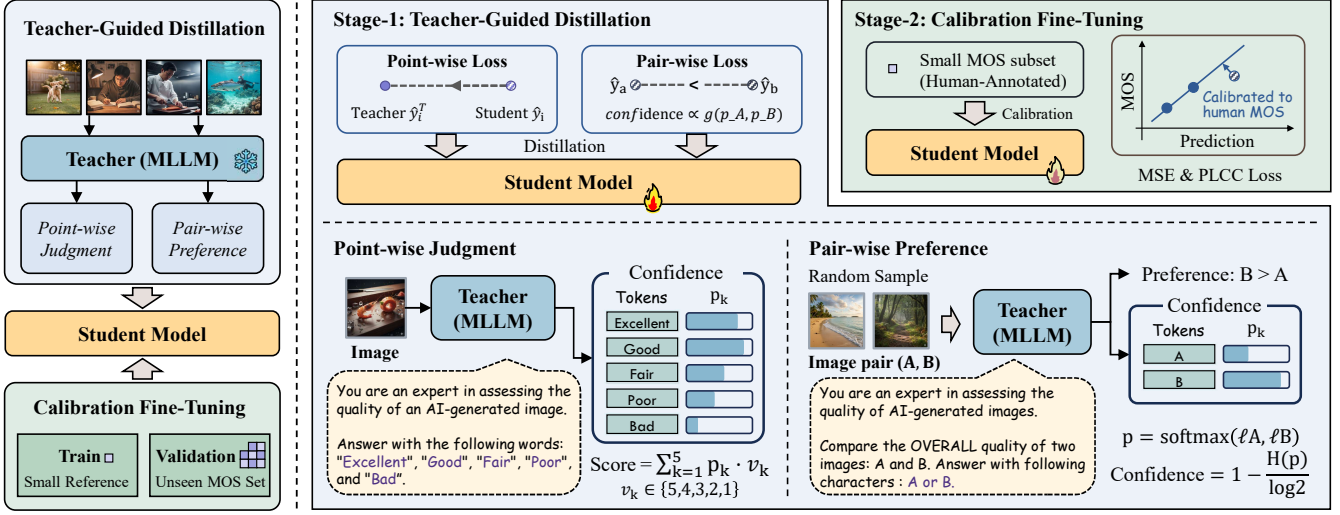
Figure 3: Overview of LEAF. Label-efficient IQA framework: Stage-1 jointly distills point-wise judgments and pair-wise preferences from an MLLM teacher into a lightweight student. Stage-2 calibrates the student to human MOS using a small annotated subset.

the student on $\mathcal{D}_{\text{MOS}}$ with regression objective together with the correlation-based objective between predictions $\{s_\theta(x_i)\}$ and MOS labels $\{y_i\}$, so that the final scores are aligned with human perceptual judgments.

3.2 Teacher-Guided Distillation (TGD)

The teacher provides two complementary supervision signals: (1) *point-wise* quality judgments for individual images, and (2) *pair-wise* preferences with confidence for image pairs. We use fixed prompt templates to ensure constrained outputs. The complete prompts are provided in the appendix.

Point-wise Judgment
For each image x, we prompt the teacher to judge its overall perceptual quality using a fixed set of discrete quality tokens $\mathcal{K} = \{Excellent, Good, Fair, Poor, Bad\}$. Instead of using the teacher's hard output, we extract token-level log-likelihoods $\{\ell_k(x)\}_{k \in \mathcal{K}}$ and convert them into a probability distribution:

$$p_k(x) = \frac{\exp(\ell_k(x))}{\sum_{j \in \mathcal{K}} \exp(\ell_j(x))}. \quad (1)$$

We then map the discrete tokens to ordinal scores $\{v_k\} = \{5, 4, 3, 2, 1\}$ (from $Excellent$ to Bad) and define a continuous teacher score by expectation:

$$\hat{y}^T(x) = \sum_{k \in \mathcal{K}} v_k\, p_k(x). \quad (2)$$

This produces a dense supervision signal for all images in $\mathcal{D}$.

Pair-wise Preference
To capture relative quality, we randomly sample pairs (x_a, x_b) and prompt the teacher to judge which image has higher quality, outputting a single token in $\{\text{A}, \text{B}\}$.

We obtain the log-likelihoods (ℓ_A, ℓ_B) at the decision position and compute:

$$p_A = \frac{e^{\ell_A}}{e^{\ell_A} + e^{\ell_B}}, \quad p_B = \frac{e^{\ell_B}}{e^{\ell_A} + e^{\ell_B}}. \quad (3)$$

The hard preference label is

$$t_{ab} = \begin{cases} 1, & \text{if teacher prefers } A\ (p_A \geq p_B), \\ 0, & \text{otherwise.} \end{cases} \quad (4)$$

Not all teacher pair-wise decisions are equally reliable. We quantify confidence through the normalized entropy of the two-class distribution:

$$H(p) = -\sum_{c \in \{A, B\}} p_c \log p_c, \qquad \omega_{ab} = 1 - \frac{H(p)}{\log 2} \in [0, 1], \quad (5)$$

where ω_{ab} is larger when teacher's decision is more certain. In practice, we discard low-confidence pairs with $\omega_{ab} < \tau$.

Distillation Objective
We distill quality prior from the teacher using dense supervision on $\mathcal{D}$. Specifically, we leverage both (i) pointwise soft scores $\hat{y}^T(x)$ and (ii) pairwise preferences $\mathcal{P}$ to train a lightweight student regressor.

Student predictor. We denote the student as an IQA regressor $s_\theta : \mathcal{X} \to \mathbb{R}$ that outputs a scalar quality score. Our formulation does not rely on a specific architecture, requiring only real-valued outputs suitable for regression and ranking.

Point-wise distillation. Given teacher-provided soft scores $\hat{y}^T(x)$ for $x \sim \mathcal{D}$, we minimize

$$\mathcal{L}_{\text{reg}} = \mathbb{E}_{x \sim \mathcal{D}} \left[\text{SmoothL1}\left(s_\theta(x), \hat{y}^T(x)\right) \right]. \quad (6)$$

Pair-wise distillation. Given teacher-provided pairs $\mathcal{P} = \{(x_a, x_b, t_{ab}, \omega_{ab})\}$, we define

$$P_\theta(a \succ b) = \sigma\left(s_\theta(x_a) - s_\theta(x_b)\right), \qquad \sigma(z) = \frac{1}{1 + e^{-z}}. \quad (7)$$

We optimize a weighted binary cross-entropy loss:

$$\mathcal{L}_{\text{rank}} = \mathbb{E}_{(x_a, x_b, t_{ab}, \omega_{ab}) \sim \mathcal{P}} \left[\omega_{ab} \cdot \text{BCE}\left(P_\theta(a \succ b), t_{ab}\right) \right]. \quad (8)$$

Joint objective. The objective of this stage is

$$\mathcal{L}_{\text{dis}} = \mathcal{L}_{\text{reg}} + \lambda_{dis}\mathcal{L}_{\text{rank}}, \qquad (9)$$

where λ_{dis} is used to balance point-wise and pair-wise distillation. We select the checkpoint without using any MOS annotations in the Mos free setting. In the few-shot setting, checkpoint selection is performed using a held-out split of the same MOS subset $\mathcal{D}_{\text{MOS}}$ that is visible for calibration fine-tuning stage, without introducing any additional labeled data or test-set leakage.

3.3 Calibration Fine-Tuning (CFT)

To align the student predictions with the human MOS scale, we fine-tune the student on the small labeled subset $\mathcal{D}_{\text{MOS}}$ with a regression and a correlation objective.

Let $\mathbf{s} = [s_\theta(x_i)]_{(x_i,y_i)\in\mathcal{D}_{\text{MOS}}}$ and $\mathbf{y} = [y_i]$ denote vectors of predictions and MOS. We first perform scale calibration using mean squared error:

$$\mathcal{L}_{\text{MSE}} = \mathbb{E}_{(x_i,y_i)\sim\mathcal{D}_{\text{MOS}}}\left[\left(s_\theta(x_i) - y_i\right)^2\right]. \qquad (10)$$

Meanwhile, we optimize the PLCC calculated within each mini-batch for differentiability by minimizing

$$\mathcal{L}_{\text{PLCC}} = 1 - \rho(\mathbf{s},\mathbf{y}), \qquad \rho(\mathbf{s},\mathbf{y}) = \frac{\text{cov}(\mathbf{s},\mathbf{y})}{\sigma(\mathbf{s})\,\sigma(\mathbf{y})}. \qquad (11)$$

The overall objective of the calibration fine-tuning stage is

$$\mathcal{L}_{\text{cal}} = \mathcal{L}_{\text{MSE}} + \lambda_{cal}\mathcal{L}_{\text{PLCC}}, \qquad (12)$$

where λ_{cal} balances absolute MOS calibration and correlation optimization.

4 Experiments

4.1 Experimental Setup

The teacher model is based on the InternVL-3.5-8B and remains frozen during all stages. We use a ConvNeXt-Base as the student model pretrained on ImageNet. All images are resized to 256 and cropped to 224×224. Random resized cropping and horizontal flipping are applied during training, while center cropping is used for evaluation. We use AdamW for model optimization and adopt mixed precision training. Stage 1 is trained jointly with the objective by using point-wise judgments and pairwise preferences provided by the teacher, where $\lambda_{dis} = 0.5$. Stage-2 fine-tunes the student on the labeled subset using a correlation-based objective to align the prediction results with human MOS. Hyperparameters and implementation details, including pair construction and filtering strategies, are provided in the supplementary material.

4.2 Datasets and Evaluation Protocol

We evaluate on the image quality assessment benchmarks for both user-generated content (UGC) and AI-generated content (AIGC). For UGC, we use KonIQ-10k [Hosu *et al.*, 2020] and SPAQ [Fang *et al.*, 2020], which contain natural images with authentic distortions from real-world capture and processing pipelines. For AIGC, we use AGIQA-3K [Li *et al.*, 2023],

Table 1: Comparison with state-of-the-art IQA methods on AIGC benchmarks.

Methods	AGIQA-3K		AIGIQA-20K	
	SRCC	PLCC	SRCC	PLCC
Supervised				
BRISQUE (TIP, 2012)	0.472	0.561	0.466	0.558
HyperIQA (CVPR, 2020)	0.850	0.904	0.816	0.832
MANIQA (CVPR, 2022)	0.861	0.911	0.850	0.887
DBCNN (TCSVT, 2020)	0.826	0.890	0.805	0.848
MUSIQ (ICCV, 2021)	0.820	0.865	0.832	0.864
StairIQA (JSTSP, 2023)	0.834	0.893	0.789	0.842
Q-Align (TOMM, 2023)	0.852	0.881	0.874	0.889
MA-AGIQA (ACMMM, 2024)	0.893	0.927	0.864	0.905
Weak-supervised				
CONTRIQUE (TIP, 2022)	0.817	0.879	0.788	0.807
Re-IQA (CVPR, 2023)	0.811	0.874	0.787	0.811
CLIP-IQA+ (AAAI, 2023)	0.844	0.894	0.833	0.854
ARNIQA (WACV, 2024)	0.803	0.881	0.778	0.792
GRepQ-D (WACV, 2024)	0.807	0.858	0.789	0.810
Ours (10% MOS)	0.841	0.899	0.839	0.878
Ours (30% MOS)	**0.868**	**0.914**	**0.860**	**0.905**
Label-free				
NIQE (ISPL, 2012)	0.523	0.566	0.208	0.337
ILNIQE (TIP, 2015)	0.609	0.655	0.335	0.455
CLIP-IQA (AAAI, 2023)	0.638	0.711	0.388	0.537
MDFS (TMM, 2024)	0.672	0.676	0.691	0.695
QualiCLIP (ArXiv, 2025)	0.667	0.735	0.679	0.694
GRepQ-Z (WACV, 2024)	0.613	0.734	0.624	0.634
DUBMA (IJCAI, 2025)	0.684	0.701	0.695	0.697
Ours	**0.749**	**0.811**	**0.696**	**0.762**

AIGIQA-20K [Li *et al.*, 2024a], which cover images generated by diverse text-to-image models with varying perceptual qualities.

To quantify label efficiency, we adjusted the MOS-visible ratio on the training split, resulting in three evaluation settings that correspond to Table 1 and Table 2.

(i) label-free: the student is trained solely with teacher supervision (e.g., predicted scores and preferences), without using any human MOS.

(ii) 10% MOS: only a randomly sampled 10% subset of training images contain MOS labels, while the remaining training samples are treated as MOS-invisible.

(iii) 30% MOS: similarly, 30% of the training images contain MOS labels.

We repeat the sampling process five times with different random seeds and report the average SRCC/PLCC values across the five runs.

Across all settings, we construct the pair-wise supervision set by uniformly sampling image pairs at random, with the number of sampled pairs matching the size of the dataset. The ablation experiment on the number of samples is provided in the supplementary material.

Metrics. We report image quality assessment metrics based on standard correlation, including SRCC and PLCC, computed on the held-out test split. Relevant definitions and specific implementation details can be found in the supplemen-

Table 2: Comparison with state-of-the-art weak-supervised and label-free IQA methods on UGC benchmarks.

Methods	KonIQ-10k		SPAQ	
	SRCC	PLCC	SRCC	PLCC
Weak-supervised				
CONTRIQUE (TIP, 2022)	0.894	0.906	<u>0.914</u>	0.919
CLIP-IQA+ (AAAI, 2023)	<u>0.895</u>	<u>0.909</u>	0.864	0.866
ARNIQA (WACV, 2024)	0.869	0.883	0.904	0.909
GRepQ-D (WACV, 2024)	0.855	0.868	0.903	<u>0.917</u>
Ours (10% MOS)	0.867	0.903	0.896	0.902
Ours (30% MOS)	**0.899**	**0.916**	**0.921**	**0.922**
Label-free				
NIQE (ISPL, 2012)	0.551	0.488	0.703	0.670
ILNIQE (TIP, 2015)	0.453	0.467	0.719	0.654
CONTRIQUE (TIP, 2022)	0.651	0.637	0.677	0.685
CL-MI (WACV, 2023)	0.664	0.653	0.701	0.701
Re-IQA (CVPR, 2023)	0.580	0.568	0.613	0.616
CLIP-IQA (AAAI, 2023)	0.695	0.727	0.738	0.735
ARNIQA (WACV, 2024)	0.746	0.762	0.788	0.797
MDFS (TMM, 2024)	0.733	0.737	0.741	0.754
GRepQ-Z (WACV, 2024)	<u>0.768</u>	<u>0.784</u>	0.823	0.839
DUBMA (IJCAI, 2025)	0.703	0.740	<u>0.834</u>	<u>0.841</u>
Ours	**0.777**	**0.801**	**0.861**	**0.867**

tary materials.

4.3 Comparison with State-of-the-Art Methods

We compare our method with representative weak-supervised and label-free IQA approaches on both AIGC and UGC benchmarks. For AIGC, we report results on AGIQA-3K and AIGIQA-20K in Table 1. For UGC, we evaluate the performance on KonIQ-10k and SPAQ in Table 2. In each case, we consider both label-free and weak-supervised settings to validate the effectiveness of the proposed method.

AIGC Benchmarks
Without using any human MOS, our method shows strong correlation with human judgments on AGIQA-3K, with an SRCC of 0.749 and a PLCC of 0.811, outperforming the strongest label-free baseline in the table (SRCC = 0.684). On AIGIQA-20K, it reaches 0.696 and 0.762 in terms of SRCC and PLCC, respectively, achieving the best SRCC among label-free competitors while exceeding the best label-free PLCC 0.697. These results indicate that teacher-driven dense supervision can transfer reliable quality perception even without human labels.

With ten percent MOS, our method achieves an SRCC of 0.841 and a PLCC of 0.899 on AGIQA-3K, and 0.839 and 0.878 on AIGIQA-20K, respectively. On AGIQA-3K, the PLCC is the highest among weak-supervised methods, while the SRCC remains close to the strongest competitor. For reference, most weak-supervised IQA methods in the table are evaluated using a large portion of MOS labels (often around 70% [Saha *et al.*, 2023; Agnolucci *et al.*, 2024; Madhusudana *et al.*, 2022]) to calibrate the regression head. In contrast, we report results with 30% MOS in our framework, with the performance on AGIQA-3K further improving to 0.868 and 0.914, and to 0.860 and 0.905 on AIGIQA-
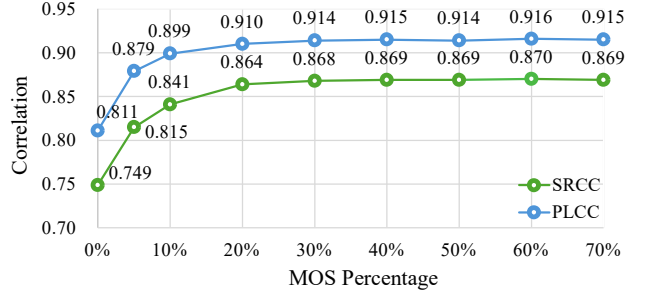

Figure 4: Impact of MOS availability during MOS calibration on AGIQA-3K.

20K in terms of SRCC and PLCC, respectively. Notably, the PLCC on AIGIQA-20K matches the best supervised result reported in the table.

UGC Benchmarks
Under the label-free setting, our method achieves strong correlations on both UGC benchmarks. On KonIQ-10k, it attains an SRCC of 0.777 and a PLCC of 0.801, while on SPAQ, it reaches 0.861 and 0.867 of SRCC and PLCC, respectively. On both datasets, our method achieved the best results among label-free competitors. In particular, on SPAQ, it improved SRCC from 0.834 to 0.861 compared to the strongest competing baseline, and in terms of PLCC, it improved from 0.841 to 0.867.

With 10% MOS, our method achieves 0.867 and 0.903 on KonIQ-10k, and 0.896 and 0.902 on SPAQ in terms of SRCC and PLCC. For reference, the compared weak-supervised methods commonly rely on around 70% of MOS labels for regression-based calibration[Madhusudana *et al.*, 2022; Saha *et al.*, 2023; Agnolucci *et al.*, 2024]. Using only thirty percent MOS, our method further improves performance to 0.899 and 0.916 on KonIQ-10k, and to 0.921 and 0.922 on SPAQ, achieving the best results among weak-supervised methods reported in Table 2. These results show that limited MOS supervision already yields strong performance, while additional MOS labels consistently improve the correlation.

4.4 Label Efficiency Analysis

Figure 4 illustrates label efficiency on AGIQA-3K by varying the MOS availability ratio in Calibration Fine-Tuning (CFT) stage while keeping Teacher-Guided Distillation (TGD) stage fixed. Overall, performance improves sharply with a small amount of MOS and then gradually saturates. Without any MOS, the model achieves an SRCC of 0.749 and a PLCC of 0.811. When the MOS ratio reaches 10%, performance increases to 0.841 and 0.899 in terms of SRCC and PLCC, respectively. As the MOS ratio further increases, the gains become marginal, reaching 0.869 and 0.915 at 30% MOS. These results indicate that CFT primarily serves to calibrate the dataset-specific score scale, enabling strong performance with limited MOS annotations.

4.5 Ablation Studies

Table 3 presents different supervision strategies used in TGD on AGIQA-3K with 10% visible MOS, including point-

Table 3: Ablation study of different supervision strategies in Teacher-Guided Distillation.

Point	Pair	Pair Conf.	SRCC	PLCC
✗	✗	✗	0.759	0.812
✓	✗	✗	0.834	0.892
✓	✓	✗	0.836	0.895
✗	✓	✓	0.829	0.889
✓	✓	✓	**0.841**	**0.899**

wise judgments, pair-wise preferences, and confidence-aware weighting on pairs.

The first row reports a CFT-only baseline, where Stage-1 distillation is removed, resulting in 0.759 and 0.812. Using only point-wise supervision to distill the teacher significantly improves the student to 0.834 and 0.892, indicating that point-wise soft judgments provide strong quality guidance. Adding pair-wise supervision on top of point-wise supervision further boosts performance to 0.836 and 0.895, showing that relative comparisons provide complementary ranking information. When relying solely on pair-wise supervision with confidence weighting, the student reaches 0.829 and 0.889. This setting still brings a noticeable performance gain, showing that pair-wise preferences can transfer useful relative quality information. However, the improvement is smaller than that achieved with point-wise supervision.

4.6 Robustness to Different Backbones

Table 4 studies the robustness of our framework to different teacher and student choices on AGIQA-3K with 10% visible MOS. Overall, stronger teachers can provide higher-quality supervision signals, and the student achieves consistent performance across various backbone network capacities.

For Qwen3-VL, SRCC and PLCC increased from 0.835 and 0.873 with the 8B model to 0.848 and 0.907 with the 32B model. Meanwhile, InternVL-3.5 provided a competitive and generally stronger supervision, reaching 0.841 and 0.899 with the 8B model and achieving the best performance of 0.850 and 0.912 with the 38B model.

For student backbones, performance improves from ResNet-18 to ConvNeXt variants, with the best performance achieved by ConvNeXt-Base with 0.841 and 0.899. Further expansion to ConvNeXt-Large does not bring additional gains, with results of 0.836 and 0.882, suggesting that a moderately sized backbone offers a better trade-off between capacity and optimization stability under the same training protocol.

5 Conclusion

In this work, we revisit the role of multimodal large language models in image quality assessment and argue that the main challenge lies not in perceptual understanding, but in aligning model outputs with dataset-specific MOS scales. Based on this insight, we propose LEAF, a label-efficient IQA framework that decouples perceptual knowledge transfer from MOS calibration. The MLLM teacher provides point-wise judgments and pair-wise preferences, while the

Table 4: Robustness to teacher models and student backbone architectures.

Setting	Params	SRCC	PLCC
MLLMs			
Qwen3-VL	8B	0.835	0.873
Qwen3-VL	32B	0.848	0.907
InternVL-3.5	8B	0.841	0.899
InternVL-3.5	38B	0.850	0.912
Student Backbones			
ResNet-18	11.7M	0.807	0.868
ResNet-50	25.6M	0.815	0.886
ConvNeXt-Tiny	28.6M	0.833	0.896
ConvNeXt-Base	88.6M	0.841	0.899
ConvNeXt-Large	197M	0.836	0.882

student model learns robust quality perception without relying on human annotations in the distillation stage. Finally, a lightweight calibration stage with a small MOS subset is sufficient to align predictions with human annotations.

Extensive experiments on both user-generated and AI-generated IQA benchmarks demonstrate that LEAF significantly reduces the dependence on annotations while achieving competitive or superior correlation with human judgments. This work provides a practical alternative to direct regression with heavy annotation requirements. We believe the proposed framework offers a promising direction for future research on label-efficient quality assessment tasks.

References

[Agnolucci et al., 2024] Lorenzo Agnolucci, Leonardo Galteri, Marco Bertini, and Alberto Del Bimbo. Arniqa: Learning distortion manifold for image quality assessment. In *2024 IEEE/CVF Winter Conference on Applications of Computer Vision (WACV)*, pages 188–197, Jan 2024.

[Agnolucci et al., 2025] Lorenzo Agnolucci, Leonardo Galteri, and Marco Bertini. Quality-aware image-text alignment for opinion-unaware image quality assessment, 2025.

[Babu et al., 2023] Nithin C Babu, Vignesh Kannan, and Rajiv Soundararajan. No reference opinion unaware quality assessment of authentically distorted images. In *2023 IEEE/CVF Winter Conference on Applications of Computer Vision (WACV)*, pages 2458–2467, Jan 2023.

[Bosse et al., 2016] Sebastian Bosse, Dominique Maniry, Thomas Wiegand, and Wojciech Samek. A deep neural network for image quality assessment. In *2016 IEEE International Conference on Image Processing (ICIP)*, pages 3773–3777, Sep. 2016.

[Chen et al., 2020] Diqi Chen, Yizhou Wang, and Wen Gao. No-reference image quality assessment: An attention driven approach. *IEEE Transactions on Image Processing*, 29:6496–6506, 2020.

[Chen *et al.*, 2024] Zewen Chen, Juan Wang, Wen Wang, Sunhan Xu, Hang Xiong, Yun Zeng, Jian Guo, Shuxun Wang, Chunfeng Yuan, Bing Li, and Weiming Hu. Seagull: No-reference image quality assessment for regions of interest via vision-language instruction tuning. *CoRR*, abs/2411.10161, 2024.

[Ding *et al.*, 2022] Keyan Ding, Kede Ma, Shiqi Wang, and Eero P. Simoncelli. Image quality assessment: Unifying structure and texture similarity. *IEEE Transactions on Pattern Analysis and Machine Intelligence*, 44(5):2567–2581, May 2022.

[Fang *et al.*, 2020] Yuming Fang, Huan Zhu, Yinan Zhang, Jinjin Li, and Kede Ma. Subjective and objective quality assessment of smartphone photography. In *Proceedings of the IEEE/CVF Conference on Computer Vision and Pattern Recognition (CVPR)*, pages 1313–1322, 2020.

[Fu *et al.*, 2024] Jun Fu, Wei Zhou, Qiuping Jiang, Hantao Liu, and Guangtao Zhai. Vision-language consistency guided multi-modal prompt learning for blind ai generated image quality assessment. *IEEE Signal Processing Letters*, 31:1820–1824, 2024.

[Hosu *et al.*, 2020] Vlad Hosu, Hanhe Lin, Tamas Sziranyi, and Dietmar Saupe. Koniq-10k: An ecologically valid database for deep learning of blind image quality assessment. *IEEE Transactions on Image Processing*, 29:4041–4056, 2020.

[Ke *et al.*, 2021] Junjie Ke, Qifei Wang, Yilin Wang, Peyman Milanfar, and Feng Yang. Musiq: Multi-scale image quality transformer. In *2021 IEEE/CVF International Conference on Computer Vision (ICCV)*, pages 5128–5137, 2021.

[Li *et al.*, 2023] Chunyi Li, Zicheng Zhang, Haoning Wu, Wei Sun, Xiongkuo Min, Xiaohong Liu, Guangtao Zhai, and Weisi Lin. Agiqa-3k: An open database for ai-generated image quality assessment. *IEEE Transactions on Circuits and Systems for Video Technology*, pages 1–1, 2023.

[Li *et al.*, 2024a] Chunyi Li, Tengchuan Kou, Yixuan Gao, Yuqin Cao, Wei Sun, Zicheng Zhang, Yingjie Zhou, Zhichao Zhang, Weixia Zhang, Haoning Wu, Xiaohong Liu, Xiongkuo Min, and Guangtao Zhai. Aigiqa-20k: A large database for ai-generated image quality assessment. In *Proceedings of the IEEE/CVF Conference on Computer Vision and Pattern Recognition (CVPR) Workshops*, pages 6327–6336, June 2024.

[Li *et al.*, 2024b] Yixuan Li, Peilin Chen, Hanwei Zhu, Keyan Ding, Leida Li, and Shiqi Wang. Deep shape-texture statistics for completely blind image quality evaluation. *ACM Trans. Multimedia Comput. Commun. Appl.*, 20(12), November 2024.

[Li *et al.*, 2025] Yunhao Li, Sijing Wu, Wei Sun, Zhichao Zhang, Yucheng Zhu, Zicheng Zhang, Huiyu Duan, Xiongkuo Min, and Guangtao Zhai. Aghi-qa: A subjective-aligned dataset and metric for ai-generated human images, 2025.

[Lin and Wang, 2018] Kwan-Yee Lin and Guanxiang Wang. Hallucinated-iqa: No-reference image quality assessment via adversarial learning. In *2018 IEEE/CVF Conference on Computer Vision and Pattern Recognition*, pages 732–741, June 2018.

[Madhusudana *et al.*, 2022] Pavan C. Madhusudana, Neil Birkbeck, Yilin Wang, Balu Adsumilli, and Alan C. Bovik. Image quality assessment using contrastive learning. *IEEE Transactions on Image Processing*, 31:4149–4161, 2022.

[Mittal *et al.*, 2012a] Anish Mittal, Anush Krishna Moorthy, and Alan Conrad Bovik. No-reference image quality assessment in the spatial domain. *IEEE Transactions on image processing*, 21(12):4695–4708, 2012.

[Mittal *et al.*, 2012b] Anish Mittal, Rajiv Soundararajan, and Alan C Bovik. Making a "completely blind" image quality analyzer. *IEEE Signal processing letters*, 20(3):209–212, 2012.

[Moorthy and Bovik, 2011] Anush Krishna Moorthy and Alan Conrad Bovik. Blind image quality assessment: From natural scene statistics to perceptual quality. *IEEE Transactions on Image Processing*, 20(12):3350–3364, Dec 2011.

[Ni *et al.*, 2024] Zhangkai Ni, Yue Liu, Keyan Ding, Wenhan Yang, Hanli Wang, and Shiqi Wang. Opinion-unaware blind image quality assessment using multi-scale deep feature statistics. *IEEE Transactions on Multimedia*, 26:10211–10224, 2024.

[Prashnani *et al.*, 2018] Ekta Prashnani, Hong Cai, Yasamin Mostofi, and Pradeep Sen. Pieapp: Perceptual image-error assessment through pairwise preference. In *2018 IEEE/CVF Conference on Computer Vision and Pattern Recognition*, pages 1808–1817, June 2018.

[Saha *et al.*, 2023] Avinab Saha, Sandeep Mishra, and Alan C. Bovik. Re-iqa: Unsupervised learning for image quality assessment in the wild. In *2023 IEEE/CVF Conference on Computer Vision and Pattern Recognition (CVPR)*, pages 5846–5855, June 2023.

[Seufert *et al.*, 2014] Michael Seufert, Sebastian Egger, Martin Slanina, Thomas Zinner, Tobias Hoßfeld, and Phuoc Tran-Gia. A survey on quality of experience of http adaptive streaming. *IEEE Communications Surveys & Tutorials*, 17(1):469–492, 2014.

[Shi *et al.*, 2024] Jinsong Shi, Pan Gao, and Jie Qin. Transformer-based no-reference image quality assessment via supervised contrastive learning. In *Proceedings of the Thirty-Eighth AAAI Conference on Artificial Intelligence and Thirty-Sixth Conference on Innovative Applications of Artificial Intelligence and Fourteenth Symposium on Educational Advances in Artificial Intelligence*, AAAI'24/IAAI'24/EAAI'24. AAAI Press, 2024.

[Shukla *et al.*, 2024] Ankit Shukla, Avinash Upadhyay, Swati Bhugra, and Manoj Sharma. Opinion unaware image quality assessment via adversarial convolutional variational autoencoder. In *2024 IEEE/CVF Winter Conference on Applications of Computer Vision (WACV)*, pages 2142–2152, Jan 2024.

[Su *et al.*, 2020] Shaolin Su, Qingsen Yan, Yu Zhu, Cheng Zhang, Xin Ge, Jinqiu Sun, and Yanning Zhang. Blindly assess image quality in the wild guided by a self-adaptive hyper network. In *2020 IEEE/CVF Conference on Computer Vision and Pattern Recognition (CVPR)*, pages 3664–3673, June 2020.

[Wang *et al.*, 2003] Z. Wang, E.P. Simoncelli, and A.C. Bovik. Multiscale structural similarity for image quality assessment. In *The Thrity-Seventh Asilomar Conference on Signals, Systems & Computers, 2003*, volume 2, pages 1398–1402 Vol.2, 2003.

[Wang *et al.*, 2023] Jianyi Wang, Kelvin C.K. Chan, and Chen Change Loy. Exploring clip for assessing the look and feel of images. *Proceedings of the AAAI Conference on Artificial Intelligence*, 37(2):2555–2563, Jun. 2023.

[Wang *et al.*, 2024] Puyi Wang, Wei Sun, Zicheng Zhang, Jun Jia, Yanwei Jiang, Zhichao Zhang, Xiongkuo Min, and Guangtao Zhai. Large multi-modality model assisted ai-generated image quality assessment. In *Proceedings of the 32nd ACM International Conference on Multimedia*, MM '24, page 7803–7812, New York, NY, USA, 2024. Association for Computing Machinery.

[Wang *et al.*, 2025a] Jiarui Wang, Huiyu Duan, Yu Zhao, Juntong Wang, Guangtao Zhai, and Xiongkuo Min. Lmm4lmm: Benchmarking and evaluating large-multimodal image generation with lmms. In *Proceedings of the IEEE/CVF International Conference on Computer Vision (ICCV)*, pages 17312–17323, October 2025.

[Wang *et al.*, 2025b] Zhihua Wang, Xuelin Liu, Jiebin Yan, Jie Wen, Wei Wang, and Chao Huang. Deep opinion-unaware blind image quality assessment by learning and adapting from multiple annotators. In *Proceedings of the Thirty-Fourth International Joint Conference on Artificial Intelligence*, IJCAI '25, 2025.

[Wen *et al.*, 2025] Wen Wen, Tianwu Zhi, Kanglong Fan, Yang Li, Xinge Peng, Yabin Zhang, Yiting Liao, Junlin Li, and Li Zhang. Self-evolving vision-language models for image quality assessment via voting and ranking. *arXiv preprint arXiv:2509.25787*, 2025.

[Wu *et al.*, 2024] Tianhe Wu, Kede Ma, Jie Liang, Yujiu Yang, and Lei Zhang. A comprehensive study of multimodal large language models for image quality assessment, 2024.

[Xu *et al.*, 2025] Zitong Xu, Huiyu Duan, Bingnan Liu, Guangji Ma, Jiarui Wang, Liu Yang, Shiqi Gao, Xiaoyu Wang, Jia Wang, Xiongkuo Min, Guangtao Zhai, and Weisi Lin. Lmm4edit: Benchmarking and evaluating multimodal image editing with lmms. In *Proceedings of the 33rd ACM International Conference on Multimedia*, MM '25, page 6908–6917, New York, NY, USA, 2025. Association for Computing Machinery.

[Xue *et al.*, 2013] Wufeng Xue, Lei Zhang, and Xuanqin Mou. Learning without human scores for blind image quality assessment. In *2013 IEEE Conference on Computer Vision and Pattern Recognition*, pages 995–1002, June 2013.

[Yang *et al.*, 2022] Sidi Yang, Tianhe Wu, Shuwei Shi, Shanshan Lao, Yuan Gong, Mingdeng Cao, Jiahao Wang, and Yujiu Yang. MANIQA: Multi-dimension Attention Network for No-Reference Image Quality Assessment . In *2022 IEEE/CVF Conference on Computer Vision and Pattern Recognition Workshops (CVPRW)*, pages 1190–1199, Los Alamitos, CA, USA, June 2022. IEEE Computer Society.

[Yuan *et al.*, 2024] Shuaiyu Yuan, Tristan Whitmarsh, Dimitri A Kessler, Otso Arponen, Mary A McLean, Gabrielle Baxter, Frank Riemer, Aneurin J Kennerley, William J Brackenbury, Fiona J Gilbert, and Joshua D Kaggie. A deep-learning-based label-free no-reference image quality assessment metric: Application in sodium mri denoising, 2024.

[Zhang *et al.*, 2011] Lin Zhang, Lei Zhang, Xuanqin Mou, and D. Zhang. Fsim: A feature similarity index for image quality assessment. *Trans. Img. Proc.*, 20(8):2378–2386, August 2011.

[Zhang *et al.*, 2015] Lin Zhang, Lei Zhang, and Alan C. Bovik. A feature-enriched completely blind image quality evaluator. *IEEE Transactions on Image Processing*, 24(8):2579–2591, Aug 2015.

[Zhang *et al.*, 2018] Richard Zhang, Phillip Isola, Alexei A. Efros, Eli Shechtman, and Oliver Wang. The Unreasonable Effectiveness of Deep Features as a Perceptual Metric . In *2018 IEEE/CVF Conference on Computer Vision and Pattern Recognition (CVPR)*, pages 586–595, Los Alamitos, CA, USA, June 2018. IEEE Computer Society.

[Zhang *et al.*, 2020] Weixia Zhang, Kede Ma, Jia Yan, Dexiang Deng, and Zhou Wang. Blind image quality assessment using a deep bilinear convolutional neural network. *IEEE Transactions on Circuits and Systems for Video Technology*, 30(1):36–47, Jan 2020.

[Zhang *et al.*, 2023] Weixia Zhang, Guangtao Zhai, Ying Wei, Xiaokang Yang, and Kede Ma. Blind image quality assessment via vision-language correspondence: A multi-task learning perspective. In *Proceedings of the IEEE/CVF Conference on Computer Vision and Pattern Recognition (CVPR)*, pages 14071–14081, June 2023.

[Zhang *et al.*, 2025] Zhichao Zhang, Xinyue Li, Wei Sun, Zicheng Zhang, Yunhao Li, Xiaohong Liu, and Guangtao Zhai. Leveraging multimodal large language models for joint discrete and continuous evaluation in text-to-image alignment. In *Proceedings of the IEEE/CVF Conference on Computer Vision and Pattern Recognition (CVPR) Workshops*, pages 977–986, June 2025.

[Zhao *et al.*, 2023] Kai Zhao, Kun Yuan, Ming Sun, Mading Li, and Xing Wen. Quality-aware pretrained models for blind image quality assessment. In *2023 IEEE/CVF Conference on Computer Vision and Pattern Recognition (CVPR)*, pages 22302–22313, June 2023.